

ARTICLE TEMPLATE

Molecular Nature of Thermodynamics and its Application to Nanosize Particle Systems

Eduardo Hernández-Huerta^a, Ruben Santamaria^a and Tomás Rocha Rinza^b

^a Departamento de Física Teórica, Instituto de Física, UNAM, México;

^b Departamento de Físicoquímica, Instituto de Química, UNAM, México.

ARTICLE HISTORY

Compiled December 2, 2021

ABSTRACT

The origins of thermodynamics from the microscopic properties of matter have not been satisfactorily accounted for. This work presents a formulation that connects Lagrangian mechanics to thermodynamics. By using such a formulation and following similar steps to those performed in the laboratory, the heat capacities, energetic and mechanical response coefficients, absorbed and emitted heats, entropy changes, and thermodynamic energies of a prototype water system, employed as an illustrative example, are found to be close to the experimental results on water bulk. The present formulation is realistic. After connecting Lagrangian mechanics to Langevin stochastic dynamics, the first law of thermodynamics is derived. The formulation not only exhibits the transformation of time-reversible equations onto time-irreversible equations, and the molecular origins of heat as well, but also reveals new pathways to investigate the thermodynamics of systems of nanometric sizes.

KEYWORDS

Lagrangian mechanics; thermodynamics; nanometric systems; free energies

1. Introduction

Thermodynamics is the field of science that deals with the different forms of energy, and their transformations. Thermodynamics is well consolidated, and has been extended to include the different states of matter, with broad applications in the industry and technology. Yet, it is regarded as a scientific branch with a primordial experimental character. On the other side, Lagrangian mechanics is the field of science that deals with the mechanical and dynamical aspects of classical objects. The modern mechanical formulations lack of providing a rational basis to thermodynamics and, in consequence, the separation between Lagrangian mechanics and thermodynamics remains in our time.

The laws of thermodynamics represent the pillars of thermodynamics. For example, the *Zero Law of Thermodynamics* establishes the heat flux from hot bodies to cold bodies to reach the thermal equilibrium, and the *First Law of thermodynamics* states that every physical system has internal energy that can be changed by the action of external factors, like mechanical work and heat. This law is different to the mechanical law of energy conservation due to the presence of the heat term in the expression of the

first law. The thermodynamic laws have empirical character [1]. Yet, we know that they have a microscopic origin, and there should be an explanation from a more fundamental theory [2]. The first attempts to link the microscopic theory to the macroscopic theory are attributed to the creators of kinetic theory [3–5]. In fact, they established the foundations of *Statistical Mechanics*, where statistical approaches are combined with (classical and quantum) mechanics to determine the properties of the macroscopic bodies with ensemble averages.

The modern simulation methods propose a Lagrangian with a bigger number of degrees of freedom than those required to describe the particle system alone, because the particle system is in contact with an environment [6]. The additional degrees of freedom may be visualized as fictitious particles capable of interacting with the real particles [7, 8]. It is through the presence of the fictitious particles that temperature and pressure effects are considered in the particle system [9, 10]. The simplifications introduced by the extended Lagrangian approaches brings some issues, and it has not been possible to deduce the first law of thermodynamics from them. A different perspective departs from the Langevin approach [11–13]. A connection between the deterministic mechanical dynamics and classical thermodynamics has not been fully achieved. An alternative form to establish the connection between microscopic and macroscopic properties employs ensemble theory [14]. It is focused in a kind of modified version of thermodynamics, which goes from the macroscopic to the microscopic behaviors of the particles [15]. In short, we have formulations that in going from the microscopic domain to the macroscopic one, and vice versa, lack of a consistent connection between the microscopic and macroscopic regimes [16].

The goal of this work is to provide an approach different to the ones currently known in the literature [17, 18] to close gaps between Lagrangian mechanics and thermodynamics. To do this, a thermodynamic prototype constituted by particles is proposed (section 2), and described using fundamental mechanics. Thus, the Lagrangian and motion equations are given in section 3. Mechanical properties such as the temperature, volume, total energy, and more, are presented in sections 4 and 5, with results of the thermodynamic observables shown in section 9. Section 15 presents the conclusions of this work. The appendixes provide details of the model interaction potentials employed in this work.

2. Microscopic thermodynamic prototype

The elements of the microscopic model are characteristic of a general (macroscopic) thermodynamic system. Such elements are: (i) the system of particles (atoms or molecules) in confinement, (ii) the container, whose atomic structure is considered in this approach, and (iii) the thermal reservoir, whose atomic structure is also considered and has interaction with the container. The system of confined particles is the relevant system of particles since we require to establish the thermodynamics of this system. There is no restriction on the container’s geometrical shape and size. The thermal reservoir is supposed to have macroscopic dimensions. The nomenclature to distinguish the types of particles is: “s” (from soup) for the particles under confinement, “x” for the particles building the container, and “q” for the particles of the environment. The molecular system to investigate is water under confinement due to the vast information we have on this system in the literature. The number of water molecules to deal with is 64 under ambient conditions of temperature ($\sim 25^\circ\text{C}$), pres-

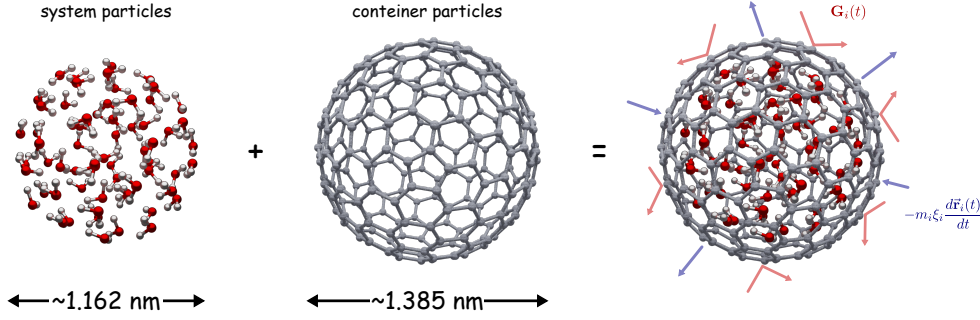


Figure 1. The microscopic prototype is characteristic of a macroscopic thermodynamic system. It is integrated by three sub-systems: (i) the (relevant) set of particles to be confined and investigated, (ii) the particles that build the container, and (iii) the particles of the heat reservoir, which are not depicted. Yet, the molecular formulation derived from the microscopic model is realistic, as the equations have universal character, and engulf the thermodynamic description of macroscopic systems.

sure (~ 1 atm), and density (1.0 g/mL). They are confined in a container of fullerene type integrated by 240 carbons, with a radius defined by the water density under ambient conditions. The container is immersed in a thermal reservoir (Fig. 1). Although the microscopic model has specific structure, geometrical shape, and size, the equations to determine in the following sections have universal nature, as they are not restricted to a given number of atoms, type of atom, or specif form of atomic arrangement. Yet, the proposed microscopic model allows to carry molecular simulations with the present computers. The following sections present the theoretical formulation and, to some extent, follow the work of Santamaria et al. [19]. The final sections provide the numerical results on the thermodynamics observables in a way of proof of principle.

3. The Lagrangian proposal

The thermodynamic model involves the confined particles (also referred to as the *system particles*), the particles of the container, and those of the heat reservoir. The Lagrangian is a functional of the individual degrees of freedom of such particles [20]:

$$\mathcal{L}(s_k, x_i, q_{ij}, \dot{s}_k, \dot{x}_i, \dot{q}_{ij}, t) = \sum_i \frac{m_i}{2} \dot{x}_i^2 + \sum_{ij} \frac{m_{ij}}{2} \dot{q}_{ij}^2 + \sum_k \frac{m_k}{2} \dot{s}_k^2 \quad (1)$$

$$- E_{qx}(\{q_{ij}, x_i\}) - E_{xs}(\{x_i, s_k\}) - E_{ext}(\{x_i, s_k\})$$

The positions s_k , x_i and q_{ij} correspond to the confined particles, container particles, and heat-bath particles, respectively. Their masses are m_k , m_i , and m_{ij} , where the indexes refer to individual particles. The mass m_{ij} carries two indexes as the j th particle of the thermal bath is in interaction with the i th particle of the container (m_{ij} should not be confused with the reduced mass). The potential energy E_{qx} provides the interactions among the heat-bath particles (of type $q - q$), and of such particles with the container particles (of type $q - x$). The potential energy E_{xs} gives the interactions among the container particles (of type $x - x$), of such particles with the confined particles (of type $x - s$), and the interactions among the confined particles (of type $s - s$). The potential energy E_{ext} represents an external field acting on the confined particles and the container particles.

The individual particles of the thermal reservoir play a second role in this investigation

because they do not interact directly with the confined system of particles. Therefore, it is convenient to introduce approximations of the energy term E_{qx} . The first step in this quest is to consider that each particle x_i has interaction with its own set of q -particles. This is a mathematically important step because it helps to uncouple the interactions among the container particles in the equations of the heat-bath particles. Yet, the separation of the heat-bath particles in sets for the x -particles is alleviated later. The harmonic approximation is used to describe the interaction of the thermal-reservoir particles with those of the container [21, 22]:

$$E_{qx} = \sum_{ij} \left[\frac{m_{ij}\omega_{ij}^2}{2} q_{ij}^2 - c_{ij}q_{ij}x_i + \frac{c_{ij}^2}{2m_{ij}\omega_{ij}^2} x_i^2 \right] \quad (2)$$

The harmonic potential E_{qx} considers the individual q and x vibrational degrees of freedom, including the coupling terms $q_{ij}x_i$ with strength c_{ij} , and the vibrational frequencies ω_{ij} [23]. The energy term E_{xs} is approximated in the framework of molecular-mechanics with a forcefield, but quantum-mechanical calculations can be similarly performed:

$$E_{xs} = U_x^{str} + U_{xs}^{vdw} + U_s^{el} + U_s^{vdw} + U_s^{str} \quad (3)$$

U_x^{str} is a potential of harmonic type for the ($x-x$ bonded) interactions of the container particles, U_{xs}^{vdw} represents the van der Waals (vdw) ($x-s$ non-bonded) interactions of the container particles and the confined particles, U_s^{el} and U_s^{vdw} stand for the Coulombic and vdw ($s-s$ non-bonded) interactions of the confined particles, and U_s^{str} is a potential of harmonic type for the ($s-s$ bonded) interactions of the individual molecules that constitute the confined particles. The details of the different interaction models are found in Appendix A.

3.1. The equations of motion

The Euler-Lagrange method gives the procedure to obtain the motion equations from the Lagrangian. The equations describe the time evolution of the three types of particles:

$$\begin{aligned} m_{ij}\ddot{q}_{ij} &= c_{ij}x_i - m_{ij}\omega_{ij}^2q_{ij} \\ m_i\ddot{x}_i &= \sum_j \left(c_{ij}q_{ij} - \frac{c_{ij}^2}{m_{ij}\omega_{ij}^2} x_i \right) - \frac{\partial E_{xs}}{\partial x_i} - \frac{\partial E_{ext}}{\partial x_i} \\ m_k\ddot{s}_k &= -\frac{\partial E_{xs}}{\partial s_k} - \frac{\partial E_{ext}}{\partial s_k} \end{aligned} \quad (4)$$

It is possible to solve the first expression analytically due to the uncoupling of the x_i particle from the other particles of type x_j ($j \neq i$) in the equations of the q_{ij} particles. The solution is inserted into the second expression [24, 25]. It can be shown that the container particles are influenced by two main terms: a memory kernel K_i and a noise source G_i [19]. In spite of that, the solutions for the container particles are still mathematically complicated to obtain. In order to reach the solutions, the kernel term is simplified by assuming a heat bath of weakly-coupled interacting oscillators, statistically described by the Debye theory. A short-time memory kernel leads to a dissipative force acting on the i th atom of the container, and the stochastic term G_i is determined by a Chandrasekhar's bivariate distribution function of the position and

velocity of the i th atom [26]. The distribution function alleviates the initial supposition on the existence of different sets of heat-bath particles for the x_i atoms of the container, because a single distribution function is applied to all the container atoms. The final expressions show the coupling of the Newtonian and Langevin equations, including the heat-bath effects in statistical manner:

$$\begin{aligned} \text{Langevin : } m_i \ddot{x}_i &= -\frac{\partial E_{xs}}{\partial x_i} - \frac{\partial E_{ext}}{\partial x_i} - m_i \xi_i \frac{dx_i(t)}{dt} + G_i(t) \\ \text{Newton : } m_k \ddot{s}_k &= -\frac{\partial E_{xs}}{\partial s_k} - \frac{\partial E_{ext}}{\partial s_k} \end{aligned} \quad (5)$$

The Langevin viscosity ξ_i and temperature T are the parameters that characterize the reservoir. The terms $-m_i \xi_i dx_i/dt$ and G_i represent accelerating and decelerating terms connected to the fluctuation-dissipation effects of the heat bath, and acting on the container particles. The last expression of Eqs. (5) describes the dynamics of the confined particles in interaction with the container particles. It keeps the deterministic nature of the Newtonian expression because we are interested on determining the thermodynamic state of the confined particles. It is important to remark that other approaches of the literature include fictitious forces on the confined particles via extended degrees of freedom in the Lagrangian, and are combined with periodic boundary conditions. The sampling of the phase space using those approaches is expected to differ from the sampling obtained with the present approach due to the existence of fictitious forces and the use of periodic boundary conditions in the other approaches. The predictions of such approaches are improved when scale factors are applied to the ensemble averages, with the purpose of compensating for the action of the fictitious forces on the real particles. In this work, there are no scale factors as the confined particles are subjected to real forces, this is, every confined particle only interacts with neighbor particles and the container.

The original Lagrangian equations of motion are time-symmetric. Nevertheless, the equations of motion of the container atoms evolved onto stochastic expressions, in turn affecting the dynamics of the confined particles. In this regard, the trajectories of the confined particles in the backwards time direction are not expected to reproduce the trajectories of the confined particles obtained in the forward time direction. This is due to the action of the stochastic forces on the container particles, which interact with the confined particles. The stochastic terms summarize the effects of a macroscopic heat bath, composed by many particles. Thus, those terms bring some issues in the formulation, like the lost of information on the system, which is the cause for no reproducing the particle trajectories discussed previously. However, this is a general feature of any formulation that introduces simplified terms, in particular, the thermodynamic theory. Finally, the set of Eqs. (5) may be also used to describe a body with atomic structure moving stochastically. This is, a *Brownian body*, whether it is microscopic or macroscopic in size, with any geometrical shape. In the limit of reducing the Brownian body to a single particle, it is possible to reproduce the stochastic dynamics of a single particle [27].

4. Mechanical temperature, confinement volume, and particle density

A *mechanical temperature*, T_{mec} , is defined in terms of the average kinetic energy of the confined particles [28]:

$$T_{mec} = \frac{2}{(3N-6)k_B} \sum_k \frac{m_k}{2} \dot{\mathbf{s}}_k^2 \quad (6)$$

The number of degrees of freedom of the confined particles is $3N-6$, and k_B is the *Boltzmann constant*. Let us also consider the statistical temperature T_{st} imposed in the laboratory through the heat bath. The thermal equilibrium is achieved when $T_{mec} = T_{st}$. In this regard, the *Zero Law of Thermodynamics* is satisfied. The simulations satisfy the *ergodic hypothesis* when: $T_{mec} = T_{st}$, and the particle dynamics allows to cover the entire phase-space that the confined particles are entitled to. In our example, the container has spherical shape, and the confined volume is:

$$V_{conf} = \frac{4}{3}\pi R_{conf}^3 \quad \Rightarrow \quad R_{conf} = R_{part} + \frac{1}{2}(R_{cage} - R_{part}) \quad (7)$$

The confining radius R_{conf} is given in terms of the radii R_{part} and R_{cage} , where R_{part} is the radius of the most external particles in confinement, and R_{cage} is the average radius of the container particles. The amount $[R_{cage} - R_{part}]/2$ is the correction factor that considers the occupied volume by the electron cloud of the most external confined particles. This last contribution is important in systems of nanometric size, becoming less important in macroscopic systems. The density of the confined system is $\rho = N/V_{conf}$, in particle/ \AA^3 . To compare the particle density with the bulk density, we use conversion factors to express ρ in g/mL:

$$\rho = \frac{NM_w}{N_A V_{conf}} \times 10^{24} \quad [\text{g/mL}] \quad (8)$$

M_w is the mass in grams of a mole of particles, N_A is the Avogadro's number, and V_{conf} is the confinement volume in \AA^3 .

5. Total energy

The present approach introduces stochastic terms in the equations of motion of the container atoms, and the total energy should be computed accordingly. To do this, the equations of motion are transformed onto energy equations [29]:

$$\begin{aligned} m_i \ddot{\mathbf{x}}_i \cdot d\mathbf{x}_i &= -\frac{\partial E_{xs}}{\partial \mathbf{x}_i} \cdot d\mathbf{x}_i - \frac{\partial E_{ext}}{\partial \mathbf{x}_i} \cdot d\mathbf{x}_i - m_i \xi_i \frac{d\mathbf{x}_i(t)}{dt} \cdot d\mathbf{x}_i + \mathbf{G}_i(t) \cdot d\mathbf{x}_i \\ m_k \ddot{\mathbf{s}}_k \cdot d\mathbf{s}_k &= -\frac{\partial E_{xs}}{\partial \mathbf{s}_k} \cdot d\mathbf{s}_k - \frac{\partial E_{ext}}{\partial \mathbf{s}_k} \cdot d\mathbf{s}_k \end{aligned} \quad (9)$$

It is convenient to separate the *conservative forces* (with nomenclature f) from the *non-conservative forces* (with nomenclature g):

$$\begin{aligned} \mathbf{f}_{x_i}^{int} &= -\frac{\partial E_{xs}}{\partial \mathbf{x}_i} \quad ; \quad \mathbf{f}_{s_k}^{int} = -\frac{\partial E_{xs}}{\partial \mathbf{s}_k} \quad ; \quad \mathbf{f}_{x_i}^{ext} = -\frac{\partial E_{ext}}{\partial \mathbf{x}_i} \quad ; \quad \mathbf{f}_{s_k}^{ext} = -\frac{\partial E_{ext}}{\partial \mathbf{s}_k} \\ \mathbf{g}_{x_i} &= -m_i \xi_i \frac{d\mathbf{x}_i(t)}{dt} + \mathbf{G}_i(t) \end{aligned} \quad (10)$$

When the elements of Eqs. (9) are added, and integrated, we obtain:

$$\begin{aligned}
& \sum_i \int_{\dot{\mathbf{x}}_i^{(0)}}^{\dot{\mathbf{x}}_i} m_i \dot{\mathbf{x}}_i \cdot d\dot{\mathbf{x}}_i + \sum_k \int_{\dot{\mathbf{s}}_k^{(0)}}^{\dot{\mathbf{s}}_k} m_k \dot{\mathbf{s}}_k \cdot d\dot{\mathbf{s}}_k = \\
& \sum_i \int_{\mathbf{x}_i^{(0)}}^{\mathbf{x}_i} \mathbf{f}_{x_i}^{int} \cdot d\mathbf{x}_i + \sum_k \int_{\mathbf{s}_k^{(0)}}^{\mathbf{s}_k} \mathbf{f}_{s_k}^{int} \cdot d\mathbf{s}_k \\
& + \sum_i \int_{\mathbf{x}_i^{(0)}}^{\mathbf{x}_i} \mathbf{f}_{x_i}^{ext} \cdot d\mathbf{x}_i + \sum_k \int_{\mathbf{s}_k^{(0)}}^{\mathbf{s}_k} \mathbf{f}_{s_k}^{ext} \cdot d\mathbf{s}_k \\
& + \sum_i \int_{\mathbf{x}_i^{(0)}}^{\mathbf{x}_i} \mathbf{g}_{x_i} \cdot d\mathbf{x}_i
\end{aligned} \tag{11}$$

The integrals involving the conservative forces are due to an ordered work, W , while the non-conservative forces characterize a *disordered work*, which is an energy in transition and is recognized as *heat*, Q :

$$\begin{aligned}
W_x^{int} &= \sum_i \int_{\mathbf{x}_i^{(0)}}^{\mathbf{x}_i} \mathbf{f}_{x_i}^{int} \cdot d\mathbf{x}_i \quad ; \quad W_s^{int} = \sum_k \int_{\mathbf{s}_k^{(0)}}^{\mathbf{s}_k} \mathbf{f}_{s_k}^{int} \cdot d\mathbf{s}_k \\
W_x^{ext} &= \sum_i \int_{\mathbf{x}_i^{(0)}}^{\mathbf{x}_i} \mathbf{f}_{x_i}^{ext} \cdot d\mathbf{x}_i \quad ; \quad W_s^{ext} = \sum_k \int_{\mathbf{s}_k^{(0)}}^{\mathbf{s}_k} \mathbf{f}_{s_k}^{ext} \cdot d\mathbf{s}_k \\
Q &= \sum_i \int_{\mathbf{x}_i^{(0)}}^{\mathbf{x}_i} \mathbf{g}_i \cdot d\mathbf{x}_i = \sum_i \int_{\mathbf{x}_i^{(0)}}^{\mathbf{x}_i} \left(-m_i \xi_i \frac{d\mathbf{x}_i(t)}{dt} + \mathbf{G}_i(t) \right) \cdot d\mathbf{x}_i
\end{aligned} \tag{12}$$

Solving the integrals on the left side of Eq. (11), and inserting expressions (12) in Eq. (11), gives:

$$\begin{aligned}
& \sum_i \left\{ \frac{m_i}{2} \dot{\mathbf{x}}_i^2 - \frac{m_i}{2} [\dot{\mathbf{x}}_i^{(0)}]^2 \right\} + \sum_k \left\{ \frac{m_k}{2} \dot{\mathbf{s}}_k^2 - \frac{m_k}{2} [\dot{\mathbf{s}}_k^{(0)}]^2 \right\} = \\
& W_x^{int} + W_s^{int} + W_x^{ext} + W_s^{ext} + Q
\end{aligned} \tag{13}$$

The internal works of Eq. (13) are defined by the difference of a potential energy function evaluated at the initial and final states:

$$W_x^{int} = E_{p,x}^{(0)} - E_{p,x} \quad ; \quad W_s^{int} = E_{p,s}^{(0)} - E_{p,s} \tag{14}$$

By using these energy differences in Eq. (13), and replacing the quantity $E_{p,x} + E_{p,s}$ by the function E_{xs} , we obtain:

$$\begin{aligned}
& \sum_i \frac{m_i}{2} \dot{\mathbf{x}}_i^2 + \sum_k \frac{m_k}{2} \dot{\mathbf{s}}_k^2 + E_{xs}(\{\mathbf{x}_i, \mathbf{s}_k\}) - \\
& \left\{ \sum_i \frac{m_i}{2} [\dot{\mathbf{x}}_i^{(0)}]^2 + \sum_k \frac{m_k}{2} [\dot{\mathbf{s}}_k^{(0)}]^2 + E_{xs}(\{\mathbf{x}_i^{(0)}, \mathbf{s}_k^{(0)}\}) \right\} \\
& = W_x^{ext} + W_s^{ext} + Q
\end{aligned} \tag{15}$$

The terms that define the *total internal energy*, E_{int} , of the whole particle system are:

$$E_{int} = \sum_i \frac{m_i}{2} \dot{\mathbf{x}}_i^2 + \sum_k \frac{m_k}{2} \dot{\mathbf{s}}_k^2 + E_{xs} \quad (16)$$

The final expression with the new nomenclature is:

$$\Delta E_{int} = E_{int} - E_{int}^{(0)} = W_x^{ext} + W_s^{ext} + Q \quad (17)$$

Eq. (17) is the *First Law of Thermodynamics*. Sekimoto carried out an analysis using a single Langevin particle and obtained a first-law like energy expression [27, 30]. That work is important as it illustrates a link between thermodynamics and stochastic dynamics. In our work we observe the same type of connection for the particles forming the container. Nevertheless, our analysis additionally includes terms of a confined system whose description is, in fact, fundamental since it includes no stochastic terms. In this form, it is possible to connect the thermodynamic theory to stochastic dynamics, and this last one to the deterministic Lagrangian dynamics of the confined system of particles.

6. Energy of confinement

It is important to obtain the *internal energy*, U , of the confined particles. Thus, the energy of the container particles is subtracted from E_{int} presented in Eq. (16):

$$U = E_k + E_p \quad ; \quad E_k = \sum_k \frac{m_k}{2} \dot{\mathbf{s}}_k^2 \quad (18)$$

$$E_p = E_{xs} - U_x^{str} = U_{xs}^{vdw} + U_s^{el} + U_s^{vdw} + U_s^{str}$$

The above internal energy is the *confining energy*. It is not conserved because the contact of the confined particles with the container brings the *thermal fluctuations* into consideration. The thermal fluctuations are significant at the microscopic level and less significant at the macroscopic one [31].

7. Parametrization of the confining energy

It is convenient to have an analytic expression of the confining energy U in terms of N , V , T . To do this, we require to carry a number of simulations using different confining volumes, and maintaining the temperature fixed: $(E_p^{(1)}, V_1, T)$, $(E_p^{(2)}, V_2, T)$, \dots , $(E_p^{(n)}, V_n, T)$. Several isotherms are generated by changing the temperature. The Vinet curve is adequate in this context [32]:

$$E_p(V, T) = a(T) + b(T) e^{\gamma(T) V^{1/3}} + c(T) V^{1/3} e^{\gamma(T) V^{1/3}} \quad (19)$$

The parameters a , b , c , and γ are obtained after fitting the Vinet curve to the required isotherm [33]. Under such conditions, an analytical internal energy of the confined particles is achieved:

$$U(N, V, T) = \frac{1}{2}(3N - 6)k_B T + E_p(V, T) \quad (20)$$

8. Mechanical pressure

The pressure registered on the confined particles is a mechanical pressure, P_{mec} , with static and dynamic contributions:

$$P_{mec} = P_s + P_d = -\frac{\partial E_p(V, T_{eq})}{\partial V} + \frac{Nk_B T_{eq}}{V} \quad (21)$$

Eq. (21) can use the analytic form of $E_p(V, T)$ given in Eq. (19):

$$P_{mec}(N, V, T) = \frac{Nk_B T_{eq}}{V} - \left(\frac{\gamma b}{3V^{2/3}} + \frac{\gamma c}{3V^{1/3}} + \frac{c}{3V^{2/3}} \right) e^{\gamma V^{1/3}} \quad (22)$$

The system pressure may consider a reference pressure $P = P_{mec} - P_0$.

9. Thermodynamics of a particle system

One of the advantages of the present formulation resides on the fact that we can follow similar steps to those performed in the laboratory for the thermodynamic characterization of the confined particle system. The challenge is to work in a kind of worst-case scenario, where the system to deal with is composed by a finite number of particles, far from the thermodynamic limit, and the particle interactions are described by effective potentials (Appendix A). The work on such a system and the realization of such steps may be also understood as a proof of principle of the present formulation.

10. Simulation of water in the liquid state

The temperature $T = 300$ K and viscosity coefficient $\xi = 5$ ps⁻¹ of the heat-bath fluid are defined before starting the simulations. The molecular model with 64 confined water molecules and a spherical container consisting of 240 carbon atoms is employed. The simulations demand average simulation times of 200 ps, with an integration step of 1 fs. The mechanical temperature T_{mec} is corroborated with the statistical temperature T_{st} of the heat bath, and the averages of the physical variables are calculated in 50 ps intervals. The radial distribution function of the oxygen atoms shows structural O...O peaks at 2.8 Å and 3.5 Å. The experimental measurements show peaks at 2.8–2.9 Å, characterizing the first-solvation shell, and a plateau between 3.5 Å and 4.5 Å, characterizing the second-solvation shell [34, 35]. The model using a finite number of water molecules shows to be consistent with the structure of the macroscopic water bulk.

As an observation, we find that the number of particles forming the container plays a second role in determining the internal energy of the confined particles. Furthermore, the ratio U_{xs}^{vdw}/U decreases when the number of confined particles increases, as expected.

11. Constant volume process

The heat capacity at constant volume is calculated with reservoir temperatures of 300, 315 and 330 K, maintaining the number of particles and volume fixed. The fluctuations

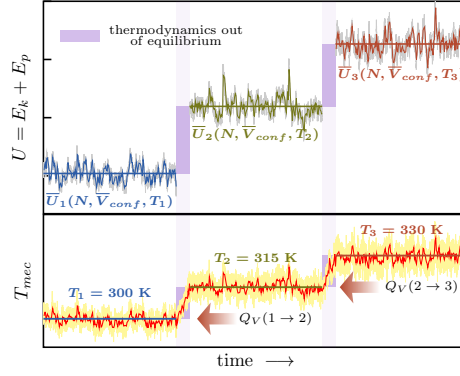


Figure 2. (i) The instantaneous internal energy and (ii) instantaneous mechanical temperature are shown. The heat-reservoir temperature is 300, 315, and 330 K for the system of 64 confined water molecules under constant volume. The values of the average energies \bar{U}_i are given in Table 1.

of the temperature and internal energy are presented in Fig. 2. The internal energy U is given by the addition of the kinetic energy E_k and potential energy E_p , Eqs. 18. The horizontal lines in Fig. 2 represent the time averages of the physical variables. The average energies are provided in Table 1. The values are similar to those using different types of methodologies in the literature [36].

The *caloric curve* is obtained from the previous data. According to the temperature range given in Table 1, the energy U is linearly related to the temperature, $U(T) = 2.03962 \times 10^{-3} T - 1.29514$ au. The differentiation of this expression with respect to T gives the heat capacity C_V . The computed value is 2.03962×10^{-3} au/K. The equivalent specific value is 4.6485 J/ (g K). The experimental value is 4.0893 J/ (g K). The computed values are in reasonable agreement with the experiment. Other theoretical values of C_V reported in the literature show larger deviations from the experimental values [37, 38].

The heat transferred to the confined system of particles to produce the temperature changes given in Table 1 is computed from $Q_V = \Delta U$, the *mechanical equivalent of heat*. In the change of states 300 K \rightarrow 315 K, and 315 K \rightarrow 330 K, the transferred heat is 1.4604 kJ/mol and 1.1281 kJ/mol, respectively. Such data is close to the experimental values 1.1294 kJ/mol and 1.1292 kJ/mol under the same temperature changes if we consider that the investigated case is considered a worst-case scenario.

Table 1. Time averages of the internal energy and its energy components using different equilibrium temperatures.*

\bar{T}_{mec} [K] (Eq. 6)	\bar{E}_p [au] (Eq. 18)	\bar{E}_k [au] (Eq. 18)	\bar{U} [au] $\bar{E}_k + \bar{E}_p$
299.4	-0.9558	0.2702	-0.6856
315.2	-0.9345	0.2845	-0.6500
330.3	-0.9206	0.2981	-0.6225

*The particle density is 1 g/mL.

Table 2. Time average properties of 64 water molecules confined in a 240 carbon-atom container.*

\bar{V}_{conf} [nm ³]	ρ [g/ml]	$T = 300$ K			$T = 315$ K			$T = 330$ K		
		\bar{E}_p	\bar{U}	P	\bar{E}_p	\bar{U}	P	\bar{E}_p	\bar{U}	P
1.9070	1.00	-0.9558	-0.6856	1.0	-0.9345	-0.6500	302.4	-0.9206	-0.6225	426.9
1.8383	1.04	-0.9498	-0.6774	2,182.4	-0.9324	-0.6471	2,587.5	-0.9100	-0.6113	2,738.1
1.7230	1.11	-0.9285	-0.6561	8,525.2	-0.9069	-0.6217	9,226.2	-0.8868	-0.5877	9,448.2
1.6178	1.18	-0.8829	-0.6110	19,841.2	-0.8574	-0.5735	21,057.6	-0.8429	-0.5455	21,399.5
1.5193	1.26	-0.7970	-0.5260	40,169.0	-0.7797	-0.4953	42,290.2	-0.7554	-0.4575	42,836.1

*The units of the potential energy \bar{E}_p , Eq. (19), and the internal energy \bar{U} , Eq. (20), are au, and of the pressure P , Eq. (22), are atm. The average kinetic energies evaluated at different temperatures are E_k (300 K)= 0.2716 au, E_k (315 K)= 0.2847 au, and E_k (330 K)= 0.2982 au. The average densities, ρ , and volumes of confinement, \bar{V}_{conf} , are also reported.

12. Constant pressure process

The calculation of the heat capacity at constant pressure, C_P , is difficult as the enthalpy is required, and the enthalpy demands knowledge of the pressure P at every equilibrium state. In order to evaluate C_P , a series of simulations with fixed temperature T , and changing the volume V_{conf} , are performed to simulate an *isothermal compression process*. Several isotherms of the type $E_p = E_p(V, T = \text{constant})$ are determined, and shown in Table 2. The use of Eq. (19) allows to parametrize E_p to reproduce the data of Table 2. The values of the parameters a , b , c , and γ of Eq. (19) are given in Table 3. After the insertion of Eq. (19) in Eq. (20), we obtain the analytic expressions of the isotherms $U_1 = U(V, T_1 = 300 \text{ K})$, $U_2 = U(V, T_2 = 315 \text{ K})$ and $U_3 = U(V, T_3 = 330 \text{ K})$ (Fig. 3).

The mechanical pressure is analytically computed from Eq. (22). Firstly, it is necessary to provide a reference pressure. The liquid state of water at 300 K and 1 atm is taken

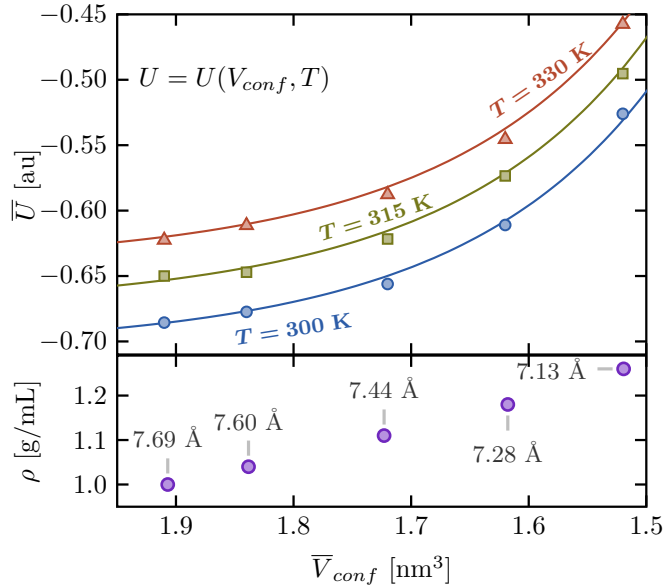


Figure 3. The average internal energy, Eq. (18), and the confinement volume, Eq. (7), are shown along the isotherms 300 K, 315 K, 330 K. The numerical data are represented by points. The curves were generated analytically after: (i) using Eq. (19) in Eq. (18) for the potential energy E_p , and (ii) fitting Eq. (19) to the E_p data. The density and confinement radius, Eq. (7), of the confined water molecules is also given for the different data points.

Table 3. Parameters of the potential energy, Eq. (19), in terms of the temperature.

T [K]	a [au]	$b/10^{10}$ [au]	$c/10^9$ [au/nm]	γ [1/nm]
300	-0.9787	6.55	6.74	-23.2678
315	-0.9605	6.55	6.74	-23.2274
330	-0.9412	6.55	6.74	-23.2123

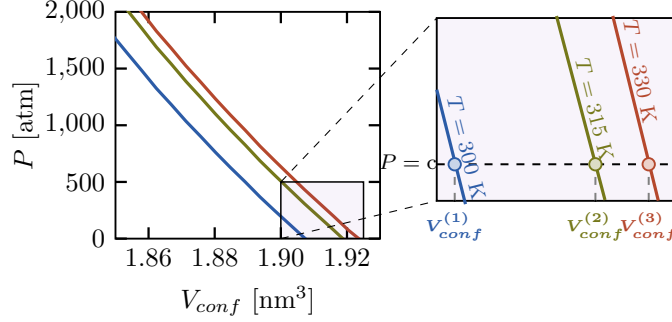


Figure 4. The P vs V curves are shown for the isotherms 300, 315, 330 K. The inset is a zoom projection of P and V . The dashed line illustrates a constant value of the pressure P .

as a reference state and, thus the difference $P = P_{mec} - P_0$ is calibrated to give 1 atm for the system with density 1.0 g/mL at 300 K. The pressure values are reported in Table 2, with $P_0 = 6,070.3$ atm.

The pressure values 1, 50 and 100 atm are in the range resulting from the compression process. We determine the confining volume and internal energy on the different isotherms to establish the enthalpy values (Fig. 4):

$$\begin{aligned}
 H_1(T_1 = 300 \text{ K}) &= U_1 + PV_{conf}^{(1)} \\
 H_2(T_2 = 315 \text{ K}) &= U_2 + PV_{conf}^{(2)} \\
 H_3(T_3 = 330 \text{ K}) &= U_3 + PV_{conf}^{(3)}
 \end{aligned} \tag{23}$$

The enthalpy values are reported in Table 4. The relation of the enthalpy to the temperature at constant pressure is found to be a linear expression, $H(T) = AT + B$, in the range of investigated temperatures. The values 20.84, 20.85, and 20.85 in units of cal/(mol K) are obtained for the pressures 1 atm, 50 atm, and 100 atm, respectively. The experimental values are 17.99 cal/(mol K) at 1 atm, and 17.89 cal/(mol K) at 100 atm [39]. There are reported values of C_P in the literature using different model potentials for the water interactions. The values of those studies show larger deviations

Table 4. The confinement volume, V_{conf} , internal energy, U , and enthalpy, H , under different conditions of temperature and pressure.*

T_{eq} [K]	V_{conf} [nm ³] (Eq. 7)			U [au] (Eq. 20)			H [au] = $U + PV_{conf}$		
	1 atm	50 atm	100 atm	1 atm	50 atm	100 atm	1 atm	50 atm	100 atm
300	1.907	1.905	1.903	-0.6854	-0.6852	-0.6850	-0.6853	-0.6830	-0.6805
315	1.918	1.917	1.915	-0.6543	-0.6541	-0.6538	-0.6542	-0.6518	-0.6494
330	1.923	1.921	1.919	-0.6216	-0.6214	-0.6212	-0.6216	-0.6192	-0.6167

*The pressure is normalized to P_0 (given in the body text). Once the pressure P and temperature T are fixed, the confinement volume V_{conf} is determined, and the internal energy is evaluated using Eq. (20). Up to four digits after the decimal point are presented with the purpose of observing differences in the energies.

from the experimental values [40–42].

With a pressure of 1 atm, we have $C_V = 4.6485 \text{ J/(g K)}$ and $C_P = 4.8400 \text{ J/(mol K)}$, and $C_P > C_V$, which is consistent with the thermodynamics relations.

13. β and κ volumetric response coefficients

The β response factor represents the volume change of the system with respect to the temperature, keeping the pressure constant. Table 4 lists the required observables to determine β with fixed pressure. The data have a non-linear trend (Fig. 5). A quadratic expression fits the data in the analyzed temperature range. Thereby, $\partial V_{conf}/\partial T = 2AT + B$, and the thermal response coefficient is $\beta(V, T) = (2AT + B)/V_{conf}(T, P = \text{constant})$. Under the thermodynamic conditions $(P, V_{conf}, T) = (1 \text{ atm}, 1.9070 \text{ nm}^3, 300 \text{ K})$, the water-bulk value of β is $0.5166 \times 10^{-3} \text{ K}^{-1}$. The experimental value is $0.2728 \times 10^{-3} \text{ K}^{-1}$, which is of the same order of magnitude for the small water cluster (recall that it is the worst-scenario case).

In order to determine the isothermal compressibility coefficient κ , Eq. (22) is employed to obtain $(\partial P/\partial V)_T$ analytically. By using the identity $(\partial V/\partial P)_T = 1/(\partial P/\partial V)_T$ [43], and inserting it in the expression of κ , we obtain:

$$\kappa(V, T) = \left[e^{\gamma V^{1/3}} \left(\frac{b\gamma^2}{9V^{1/3}} + \frac{c\gamma^2}{9} - \frac{2b\gamma}{9V^{2/3}} - \frac{2c}{9V^{2/3}} \right) + \frac{Nk_B T_{eq}}{V} \right]^{-1} \quad (24)$$

The parameters b , c , and γ are known from Table 3. By using κ of Eq. (24), and providing values of the temperature and confining volume, the factor κ is evaluated. When $T = 300 \text{ K}$ and $V_{conf} = 1.907 \text{ nm}^3$, we have $\kappa = 0.1993 \text{ GPa}^{-1}$. The experimental value is 0.4511 GPa^{-1} . We emphasize that the system of this work is a worst-scenario case, because it is sufficiently small with respect to the size of a bulk system.

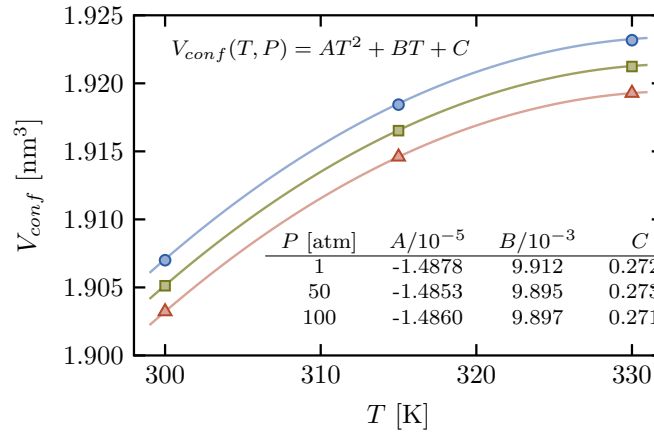


Figure 5. The confinement volume V_{conf} as a function of the temperature T is shown. The interpolating curves match the numerical data. The fitting coefficients A [nm^3/K^2], B [nm^3/K], and C [nm^3] are shown for different pressure values.

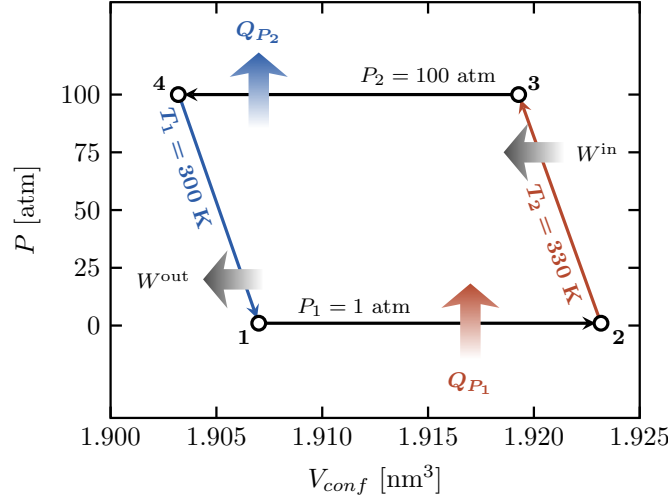


Figure 6. PV diagram of a proposed thermodynamic cycle. The arrows indicate the exchange of work and heat of the confined particle system with the heat reservoir.

14. Entropy and thermodynamic potentials

The following goal is to evaluate the changes of the internal energy U , enthalpy H , and entropy S in a cyclic thermodynamic process, which involves changes of P , V_{conf} and T . The thermodynamic cycle consists of four stages illustrated in the PV diagram of Fig. 6. The isothermal curves are essentially straight lines and $P = AV_{conf} + B$. The values of the independent variables and energy functions are given in Table 5.

The values of U and H are available from the previous calculations, and the changes of U and H in the thermodynamic cycle are directly computed, $\Delta U = U_f - U_i$ and $\Delta H = H_f - H_i$. For constant pressure processes, the enthalpy changes ΔH_{12} and ΔH_{34} correspond to the heat Q_{P1} absorbed by the system in process $1 \rightarrow 2$, and to the heat Q_{P2} released by the system in process $3 \rightarrow 4$, respectively. According to classical thermodynamics, it is possible to estimate the entropy changes ΔS in terms of the mechanical response factors. Table 6 shows the changes of U , H , and S in the four processes of the cycle. The total change of internal energy in the closed thermodynamic cycle is basically zero, and similarly in the case of ΔH and ΔS , a characteristic of *state functions* in thermodynamics. The estimates using the NIST information (Appendix B) are also provided there.

As it can be observed from the results of Table 6, the small energies (below 1 kJ/mol

Table 5. Physical observables of the thermodynamic cycle schematized in Fig. 6.*

macroscopy property	thermodynamic states			
	1	2	3	4
P [atm]	1	1	100	100
T [K]	300	330	330	300
V_{conf} [nm ³]	1.907	1.923	1.919	1.903
E_p [au]	-0.9570	-0.9199	-0.9195	-0.9565
U [au]	-0.6854	-0.6216	-0.6212	-0.6850
H [au]	-0.6853	-0.6216	-0.6167	-0.6805

*Up to four digits after the decimal point are presented with the purpose of observing differences in the energies.

Table 6. Changes of U , H and S in the thermodynamic cycle of Fig. 6.*

process	ΔU [kJ/mol]	ΔH [kJ/mol]	ΔS [J/(mol K)]
1 \rightarrow 2	2.616 (2.259)	2.616 (2.259)	8.310 (7.175)
2 \rightarrow 3	0.017 (0.335)	0.198 (0.153)	-0.009 (-0.092)
3 \rightarrow 4	-2.626 (-2.248)	-2.618 (-2.246)	-8.314 (-7.134)
4 \rightarrow 1	-0.017 (-0.346)	-0.196 (-0.166)	0.093 (0.051)
total	0.010 (0.000)	0.00 (0.000)	0.080 (0.000)

*The values in parenthesis are deduced from the NIST thermodynamic data, Table 8. From such data, the internal energy change is calculated in the form $\Delta U = \Delta H - \Delta(PV)$. For example for the process 1 \rightarrow 2, we have $U_2 - U_1 = (H_2 - H_1) - (P_2V_2 - P_1V_1)$. Refer to Sect. 14 for the discussion on the values in a gray background.

and denoted with a gray background) show differences with the values obtained from the NIST information. Such deviations are associated to two main factors: (i) the TIP3P force field of water is known to have a limited prediction of the energies, specially when the particle system is subjected to different temperatures [44, 45], and (ii) in the process of doing energy fittings (with the purpose of obtaining analytical expressions of certain energies), small deviations between the predicted energies from the analytical expressions and the numerical energies occur. In consequence, the accumulation of such deviations may be the reason to obtain energy differences smaller than 1 kJ/mol. Note that 1 kJ/mol is lower than the chemical accuracy expected, for example, from density functional theory. In this regard, the small energies of Table 6 should be interpreted with care, and the deviations should not be associated to the formulation of this work because the numerical energies may be improved under the use of better force fields or accurate methods of electronic structure theory.

The changes of free energies ΔF and ΔG are obtained after integrations of P and V , respectively. The integration of P is performed using the analytic form of the pressure in terms of the volume:

$$\Delta F = \Delta E_p - Nk_B T_{mec} \ln \left(\frac{V_2}{V_1} \right) \quad (25)$$

In the case of the Gibbs energy, we require the inverse function $V = V(P, T)$, which is generated from the data of Table 4. Instead of using the state functions $P = P(V, T)$ and $V = V(P, T)$, the free energy changes may be alternatively computed from ΔU ,

Table 7. Free energy changes and pressure along the isothermal curves of the thermodynamic cycle of Fig. 6.*

free energies [kJ/mol]		2 \rightarrow 3 (330 K)	4 \rightarrow 1 (300 K)
ΔF	NIST	0.3654	-0.3613
	$\Delta F = - \int_i^f P dV$	0.1870	-0.1815
ΔG	NIST	0.1834	-0.1813
	$\Delta G = \int_i^f V dP$	0.1814	-0.1798
$P = AV_{conf} + B$			
A [atm/nm ³]		-2.6225×10^4	-2.5450×10^4
B [atm]		5.0013×10^4	4.8946×10^4

*The expression of P reproduces the pressure in going from state 2 to state 3, and from state 4 to state 1 of the thermodynamic cycle. The values of A and B are computed from data of Table 4.

ΔH , and ΔS , and the listed values of Table 6. The values of ΔF and ΔG for the isothermal processes $2 \rightarrow 3$ and $4 \rightarrow 1$ of the thermodynamic cycle are shown in Table 7 and compared with those generated from the NIST data.

It is important to mention that the formulation of this work gives foundation to previous molecular models where: (i) the results on highly pressurized hydrogen clusters have shown excellent agreement with the experimental results using diamond anvil cells [46], and (ii) a single electron (an elementary particle) was confined in a spherical cage of He atoms, showing the localized and delocalized states of the electron by simply changing the cage radius, thus exhibiting the wave-particle duality of the electron by changing a single parameter in the simulation [47].

15. Conclusions

The formulation presented in this work combines a Lagrangian description of the confined atoms in interaction with the container atoms, and a Langevin description of the container atoms in interaction with the heat bath. The combination of such levels of theory takes us from an original set of expressions, where all of them are deterministic, to a subset of equations where the deterministic character is maintained for the confined atoms, and another subset of equations where the initial expressions have been transformed onto stochastic equations of motion for the atoms forming the container. All the equations of motion are coupled together, and have universal character as they are not restricted to a given number of atoms, type of atom, or specific form of atomic arrangement. In this quest the molecular nature of thermodynamics is exhibited, and confirmed by reproducing the known features of heat, the first law of thermodynamics, and allowing to introduce in mechanical form the energetic and mechanical response coefficients, pressure, amount of heat transfer, entropy, and free energies of the system of confined particles. In this respect, the formulation is different to other approaches reported in the literature. The numerical results on a thermodynamic prototype, intentionally designed to be a worst-scenario case due to its small size, use of moderate forcefields, and influence of the border effects, are relatively close to the experimental measurements on water bulk. The present formulation gives the possibility of obtaining thermodynamic properties of systems of nanometric sizes from molecular simulations by simply imitating the ordinary measurement steps performed in the laboratory. The formulation may be also used to investigate systems far from thermodynamic equilibrium due to the general nature of molecular dynamics. Preliminary results on the application of this formulation in fluid dynamics has shown excellent results.

16. Acknowledgments

RS and EHH thank DGTIC-UNAM for access to the Miztli-UNAM computer, and express gratitude to Carlos E. Lopez Nataren and the staff of IF-UNAM for helping with the computations. RS and EHH acknowledge PAPIIT-DGAPA (Project Num. IN-111-918) for financial support.

17. Appendix A: model interaction potentials

The model potentials that simulate the interactions of the confined particles and the container particles are described in this section. The model potentials are contributions to the energy E_{xs} , Eq. (3).

17.1. Potential energy of the container atoms

The interactions among the atoms are considered of harmonic type. Consider atom 1, whose bonded neighbors are atoms 2, 3, and 4, with positions \mathbf{x}_2 , \mathbf{x}_3 , and \mathbf{x}_4 . The antipodal atom to atom 1 is atom 5, with position \mathbf{x}_5 . The potential energy of atom 1 in interaction with the other atoms is:

$$U^{str}(\mathbf{x}_1) = \frac{1}{2} k_{bond} [(|\mathbf{x}_2 - \mathbf{x}_1| - r_0)^2 + (|\mathbf{x}_3 - \mathbf{x}_1| - r_0)^2 + (|\mathbf{x}_4 - \mathbf{x}_1| - r_0)^2] + \frac{1}{2} k_{dist} (|\mathbf{x}_5 - \mathbf{x}_1| - R_0)^2 \quad (26)$$

The total potential energy of the container is obtained by addition of potentials of the above type, $U_x^{str} = U^{str}(\mathbf{x}_1) + U^{str}(\mathbf{x}_2) + U^{str}(\mathbf{x}_3) + \dots$. The container radius was reduced in different simulations, resulting in changes of the interatomic equilibrium distances r_0 and R_0 , but maintaining the same spring stiffness k_{bond} and k_{dist} of the bonded atoms and the antipodal atom, respectively. The equilibrium distances used in the simulations for r_0 are 1.73, 1.72, 1.69, 1.65, and 1.62 in Å, while for R_0 they are 17.83, 17.64, 17.30, 16.95, 16.60 in Å. The magnitude of the spring stiffness between both the bonded atoms and the antipode atoms is 1066.737 and 43.926 in kcal/(mol Å²), respectively.

17.2. Potential energy of the container-confined atoms

The interactions of the container atoms and the confined atoms are simulated with the van der Waals (*vdw*) potential. Consider the container atom 1 with position \mathbf{x}_1 as a reference atom, and an arbitrary water molecule with atoms O, H₂, H₃ and positions \mathbf{s}_1 , \mathbf{s}_2 , and \mathbf{s}_3 . The interaction energy of the reference atom with that water molecule is:

$$U^{vdw}(\mathbf{x}_1, \mathbf{s}_1, \mathbf{s}_2, \mathbf{s}_3) = 4\epsilon_{CO} \left[\left(\frac{\sigma_{CO}}{|\mathbf{x}_1 - \mathbf{s}_1|} \right)^{12} - \left(\frac{\sigma_{CO}}{|\mathbf{x}_1 - \mathbf{s}_1|} \right)^6 \right] + 4\epsilon_{CH} \left[\left(\frac{\sigma_{CH_1}}{|\mathbf{x}_1 - \mathbf{s}_2|} \right)^{12} - \left(\frac{\sigma_{CH_1}}{|\mathbf{x}_1 - \mathbf{s}_2|} \right)^6 \right] + 4\epsilon_{CH} \left[\left(\frac{\sigma_{CH_2}}{|\mathbf{x}_1 - \mathbf{s}_3|} \right)^{12} - \left(\frac{\sigma_{CH_2}}{|\mathbf{x}_1 - \mathbf{s}_3|} \right)^6 \right] \quad (27)$$

The *vdw* potential contains two parameters per atomic pair, they are ϵ_{CO} and σ_{CO} for the C \cdots O interaction, and whose values in that order are 0.1039 kcal/mol and 3.372 Å, and ϵ_{CH} and σ_{CH} for the C \cdots H interaction with values of 0.0256 kcal/mol and 2.640 Å. [48] The interactions of the container atom 1 with all the confined water molecules are obtained by addition of the potentials of the above type,

$U^{vdw}(\mathbf{x}_1, \{\mathbf{s}_k\}) = 4\epsilon \sum_k [(\sigma/|\mathbf{x}_1 - \mathbf{s}_k|)^{12} - (\sigma/|\mathbf{x}_1 - \mathbf{s}_k|)^6]$. The total interaction energy of the container with the confined particles is obtained by summing the interactions over all the container atoms, $U_{xs}^{vdw} = U^{vdw}(\mathbf{x}_1, \{\mathbf{s}_k\}) + U^{vdw}(\mathbf{x}_2, \{\mathbf{s}_k\}) + \dots$.

17.3. Potential energy of the confined atoms

The potential energy of the confined particles is due to the intramolecular energy and the intermolecular energy. The intramolecular energy is simulated by harmonic potentials. Consider a water molecule whose atoms have positions \mathbf{s}_1 , \mathbf{s}_2 , and \mathbf{s}_3 . The intramolecular energy of that molecule is:

$$U^{str}(\mathbf{s}_1, \mathbf{s}_2, \mathbf{s}_3) = \frac{1}{2} k_{OH} (|\mathbf{s}_1 - \mathbf{s}_2| - r_{OH_1})^2 + \frac{1}{2} k_{OH} (|\mathbf{s}_1 - \mathbf{s}_3| - r_{OH_2})^2 + \frac{1}{2} k_{HOH} [\theta(\mathbf{s}_1, \mathbf{s}_2, \mathbf{s}_3) - \theta_{HOH}]^2 \quad (28)$$

The first two terms include the harmonic stretching of bonds OH_1 and OH_2 , and the last term describes the harmonic stretching of the angle HOH . The equilibrium distances are r_{OH_1} and r_{OH_2} , with $r_{OH_1} = r_{OH_2} = 0.9572 \text{ \AA}$. The θ_{HOH} equilibrium angle is 104.52 Deg . The respective force constants are k_{OH_1} , k_{OH_2} , with $k_{OH_1} = k_{OH_2} = 1207.0720 \text{ kcal}/(\text{mol } \text{\AA}^2)$, and $k_{HOH} = 150.0998 \text{ kcal}/(\text{mol } \text{Rad}^2)$. The values of these parameters correspond to the TIP3P water model [49]. For the N confined water molecules, we have the total intramolecular potential energy $U_s^{str} = U^{str}(\mathbf{s}_1, \mathbf{s}_2, \mathbf{s}_3) + U^{str}(\mathbf{s}_4, \mathbf{s}_5, \mathbf{s}_6) + \dots$.

The intermolecular potential has electrostatic and van der Waals contributions. The electrostatic interaction is due to nonbonded charged atoms:

$$U_s^{el} = \frac{1}{2} \sum_{i,j} k_c \frac{q_i q_j}{|\mathbf{s}_i - \mathbf{s}_j|} \quad ; \quad i \neq j \quad (29)$$

The indexes i and j run over atoms of different water molecules. The potential is the TIP3P water coulombic potential with parameters q_H , q_O and k_c , and values of $+0.417e$, $-0.834e$, and $332.0595 \text{ (kcal/mol)} (\text{\AA}/e^2)$. The other contribution is due to the interaction of the electric dipoles of the water molecules. It is simulated using a TIP3P-water vdw potential. The parameters for the $O \cdots O$ interaction are ϵ_{OO} and σ_{OO} , with values in that order of 0.1521 kcal/mol and 3.1507 \AA [49].

$$U_s^{vdw} = 4\epsilon_{OO} \sum_{i,j} \left[\left(\frac{\sigma_{OO}}{|\mathbf{s}_i - \mathbf{s}_j|} \right)^{12} - \left(\frac{\sigma_{OO}}{|\mathbf{s}_i - \mathbf{s}_j|} \right)^6 \right] \quad (30)$$

18. Appendix B: thermodynamic data from NIST

Each of the four thermodynamic states in the cycle of Fig. 6 is defined by the temperature and pressure. Table 8 gives V , H , and S in terms of the temperatures and pressures.

Table 8. Thermodynamic properties of bulk water from the NIST data.*

State	T [K]	P [atm]	V [cm ³ /g]	H [J/mol]	S [J/(mol K)]
1	300	1	1.004	2040.8	7.1
2	330	1	1.016	4300.2	14.3
3	330	100	1.011	4452.9	14.2
4	300	100	0.999	2206.5	7.1

Refer to [50]

References

- [1] F. Mandl, in (John Wiley & Sonds, England, 1988), Chap. 1, 2nd ed., pp. 19–22.
- [2] F.W. Sears and G.L. Salinger, in (Addison-Wesley Publishin Company, United States of America, 1982), Chap. 9, pp. 250–271.
- [3] G.K. Mikhailov, in (, , 2005), Chap. 9, pp. 131–142.
- [4] J.C. Maxwell, Phil. Mag. **19**, 19–32 (1860).
- [5] A. Ben-Naim, in (World Scientific Publishing, United States of America, 2010).
- [6] W.G. Hoover, Phys. Rev. A **31**, 1695–1697 (1985).
- [7] H.C. Andersen, J. Chem. Phys. **72** (4), 2384–2393 (1980).
- [8] L. Rondoni, in , edited by Piotr Garbaczewski and Robert Olkiewicz (Springer, Germany, 2002; Available at [Lecture Notes in Physics](#)), Vol. 597, Chap. 3, pp. 35–61, Available at [Lecture Notes in Physics](#).
- [9] S. Nosé, J. Chem. Phys. **81** (1), 511–519 (1984).
- [10] S. Nosé, Mol. Phys. **52** (2), 255–268 (1984).
- [11] K. Sekimoto, in (Springer, Berlin Heidelberg, 2010; Available at [Lecture Notes in Physics](#)), Available at [Lecture Notes in Physics](#).
- [12] M. Yaghoubi, M.E. Foulaadvand, A. Berut and J. Luczka, J. Stat. Mech. **2017**, 113206 (2017).
- [13] U. Seifert, Rep. Prog. Phys. **75** (12), 126001 (2012).
- [14] C.V. den Broeck and M. Esposito, Physica A **418**, 6–16 (2015).
- [15] T.L. Hill, in (Dover Publications, INC., New York, 1994).
- [16] W.M. Haddad, Entropy **19** (11), 621 (2017).
- [17] T.L. Hill, Nano Lett. **1** (5), 273–275 (2001).
- [18] D. Bedeaux, S. Kjelstrup and S.K. Schnell, in (PoreLab, Center of Excellence, Noruega, 2020), 1st ed.
- [19] R. Santamaria, A.A. de la Paz, L. Roskop and L. Adamowicz, J. Stat. Phys **164**, 1000–1025 (2016).
- [20] H. Goldstein, in (Addison–Wesley Publishing Company, United States of America, 1981), Chap. 2, 2nd ed., pp. 35–54.
- [21] A. Caldeira and A. Leggett, Physica A **121** (3), 587–616 (1983).
- [22] F. Haake and R. Reibold, Phys. Rev. A **32**, 2462 (1984).
- [23] P. Ullersma, Physica **32** (1), 27–55 (1983).
- [24] D.G. Zill, in (Cengage Learning, United States of America, 2016), Chap. 4, 9th ed., pp. 159–165.
- [25] R. Zwanzing, in (Oxford University Press, United States of America, 2016), Chap. 1, 3rd ed., pp. 21–24.
- [26] S. Chandrasekhar, Rev. Mod. Phys. **15** (1), 1–89 (1943).
- [27] K. Sekimoto, Prog. Theor. Phys. Suppl. **130**, 17–27 (1998).
- [28] M.P. Allen and D.J. Tildesley, in (Oxford University Press, United Kingdom, 2017), Chap. 2, 2nd ed., pp. 62–66.
- [29] M. Alonso and E.J. Finn, in (Addison-Wesley Series in Physics, United States of America, 1967), Vol. 1, Chap. 9, pp. 247–248.
- [30] K. Sekimoto, J. Phys. Soc. Jpn. **66**, 1234–1237 (1997).

- [31] C. Bustamante, J. Liphardt and F. Ritort, *Phys. Today* **58** (7), 43–48 (2005).
- [32] P. Vinet, J. Ferrante, J.R. Smith and J.H. Rose, *J. Phys. C: Solid State Physics* **19** (20), L467–L473 (1986).
- [33] R. Santamaria, J.A. Mondragón-Sánchez and X. Bokhimi, *J. Phys. Chem. A* **116** (14), 3673–3680 (2012).
- [34] A.K. Soper and M.A. Ricci, *Phys. Rev. Lett.* **84**, 2881–2884 (2000).
- [35] L.G.M. Pettersson and A. Nilsson, *J. Non-Cryst. Sol.* **407**, 399–417 (2015).
- [36] E.G. Noya, C. Vega, L.M. Sese and R. Ramirez, *J. Chem. Phys.* **131**, 124518 (2009).
- [37] F. Paesani, W. Zhang, D.A. Case, T.E.C. III and G.A. Voth, *J. Chem. Phys.* **125**, 184507 (2006).
- [38] M. Shiga and W. Shinoda, *J. Chem. Phys.* **123**, 134502 (2005).
- [39] G.S. Kell, *J. Chem. Eng. Data* **20** (1), 97–105 (1975).
- [40] Y. Wu, *J. Chem. Phys.* **124**, 024503 (2004).
- [41] J.L.F. Abascal and C. Vega, *J. Chem. Phys.* **123**, 234505 (2005).
- [42] M.M.C. C. Vega, C. McBride, J.L.F. Abascal, E.G. Noya, R. Ramirez and L.M. Sese, *J. Chem. Phys.* **132**, 046101 (2010).
- [43] H.B. Callen, in (John Wiley & Sons, United States of America, 1985), Chap. 7, 2nd ed., pp. 176–189.
- [44] C. Vega and J.L.F. Abascal, *Phys. Chem. Chem. Phys.* **13**, 19663–19688 (2011).
- [45] S. Izadi and A.V. Onufriev, *J. Chem. Phys.* **145** (7), 074501 (2016).
- [46] R. Santamaría and J. Soullard, *Chem. Phys. Lett.* **414** (4–6), 483–488 (1983).
- [47] R. Santamaria, J. Soullard and R.G. Barrera, *J. Low Temp. Phys.* **195**, 96–115 (2019).
- [48] Y. Wu and N.R. Aluru, *J. Phys. Chem. B* **117** (29), 8802–8813 (2013).
- [49] W.L. Jorgensen, J. Chandrasekhar, J.D. Madura, R.W. Impey and Klein, *J. Chem. Phys.* **79** (2), 926–935 (1983).
- [50] J.M.W. Chase, *J. Phys. Chem. Ref. Data Monograph* **9**, 1–1951 (1998).